The ear as a location for wearable vital signs monitoring

32nd Annual International Conference of the IEEE EMBS
Buenos Aires, Argentina, August 31 - September 4, 2010

The Ear as a Location for Wearable Vital Signs Monitoring

David Da He, Eric S. Winokur, Thomas Heldt, and Charles G. Sodini

Abstract— **Obtaining vital signs non-invasively and in a wearable manner is essential for personal health monitoring. We propose the site behind the ear as a location for an integrated wearable vital signs monitor. This location is ideal for both physiological and mechanical reasons. Physiologically, the reflectance photoplethysmograph (PPG) signal behind the ear shows similar signal quality when compared to traditional finger transmission PPG measurements. Ballistocardiogram (BCG) can be obtained behind the ear using 25mm×25mm differential capacitive electrodes constructed using fabric. The BCG signal is able to provide continuous heart rate and respiratory rate, and correlates to cardiac output and blood pressure. Mechanically, the ear remains in the same orientation relative to the heart when upright, thus simplifying pulse transit time calculations. Furthermore, the ear provides a discreet and natural anchoring point that reduces device visibility and the need for adhesives.**

I. Introduction

VITAL signs such as heart rate, blood pressure, cardiac output, and blood oxygenation are necessary in determining the overall health of a patient. Continuous monitoring of these vital signs can help identify a patient's risk for stroke, heart attack, heart failure, arterial aneurysm, and renal failure [1].

In 2007, the United States spent over $1.1 trillion in health care expenditures on hospital care and clinical services [2]. This cost can be significantly reduced by moving routine monitoring out of the clinical setting and into the patient's home. It is estimated that home monitoring can improve false positive detection of heart failure patients and save up to $6 billion per year in the U. S. [3].

To gain patient acceptance at home, vital signs monitors must be wearable. Currently, heart monitoring is usually done by Holter monitors, which continuously measure the electrocardiogram (ECG) from the chest. Although wearable for the short term, Holter monitors use adhesives and wet electrodes that cause skin irritation, making them impractical for long term wear [4].

For blood pressure monitoring, the gold standard requires a mercury sphygmomanometer and trained personnel to detect the Korotoff sounds using a stethoscope. Although accurate, this measurement usually takes place in a clinical setting and is conducted infrequently despite the fact that blood pressure can vary up to 30% throughout the day [5]. Automatic blood pressure monitors exist for home use, but they also use a cuff which temporarily cuts off blood flow to the arm or the hand, which makes this method unsuitable for continuous blood pressure monitoring [6].

Over the past few years, several groups have worked on wearable and continuous blood pressure monitors based on pulse transit time (PTT) [7][8]. Such devices are worn at the wrist or the hand, thus requiring continuous calibration due to the changing hydrostatic pressure relative to the heart [9]. Placing a device on extremities makes it susceptible to motion artifacts that further decrease the measurement accuracy [9].

A method that is correlated to cardiac output is ballistocardiography (BCG), which is a measure of the body's reaction force to the blood expelled by the heart [10][11]. However, most BCG measurement systems involve a chair, bed, or a scale which do not allow continuous and wearable monitoring [11]-[13].

To measure blood oxygenation, a photoplethysmograph (PPG) is typically obtained through an optical transmission measurement at the finger or the ear lobe [14]. Both locations are non-rigid and yield significant motion artifacts. Reflectance PPG has been shown to be feasible on the forehead due to its reflective bony structure [15]. Unfortunately, the forehead is an impractical location for a long term wearable device due to low patient acceptance.

To address these issues, we propose the site behind the ear as a location for an integrated wearable vital signs monitor. This site is superior for both physiological and mechanical reasons. Physiologically, the bony structure behind the ear and above Reid's base line is optimal for reflectance PPG. The same location also contains BCG signal, which yields heart rate and respiratory rate, and correlates to cardiac output and blood pressure. Mechanically, the ear remains in the same orientation relative to the heart when upright, which reduces the need for complex calibrations when calculating PTT [14]. The ear location is discreet because a small device can be concealed by the ear and hair. Furthermore, as proven by hearing aids and headsets, the ear provides a natural anchoring point. This can lead to device attachment without the use of adhesives, thus further encouraging patient acceptance.

II. Reflectance PPG From Behind the Ear

Reflectance PPG is sensed behind the ear with a front-end circuit that uses the OPT101 chip, which contains a photodetector and a transimpedance amplifier in a single package. The light source for the PPG measurement is a surface mount red (660nm) LED with a viewing angle of 30°, an intensity of

Manuscript received April 23, 2010. This work was supported in part by Texas Instruments, the MIT Center for Integrated Circuits and Systems, and the Canadian NSERC Scholarship.

D. He, E. S. Winokur, T. Heldt, and C. G. Sodini are with the Department of Electrical Engineering and Computer Science, Massachusetts Institute of Technology, Cambridge, MA, 02139 USA (e-mail: davidhe@mit.edu, ewinokur@mit.edu, thomas@mit.edu, sodini@mtl.mit.edu)

32mcd, and a forward voltage of 1.72V. The amplified photodetector is capacitively coupled to a second amplifier with a gain of -110 and a bandpass frequency range of 0.18Hz to 34Hz. Finally, the output is low-pass filtered in MATLAB with a cutoff frequency of 40Hz. Fig. 1 shows the schematic of the PPG front-end circuit.

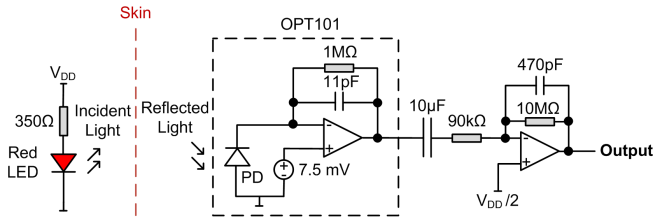

Fig. 1. The reflectance PPG front-end circuit diagram.

In order to verify the reflectance PPG measurement, transmission PPG is taken with a Criticare Systems 504-US from the left index finger and a chest ECG is taken in lead II configuration. The delay between the PPG peak and the R peak is shorter with the right ear reflectance measurement (243ms±8.0ms) when compared to the finger transmission measurement (318ms±4.6ms) because the ear is physically closer to the heart than the finger. Fig. 2 shows the three concurrent measurements.

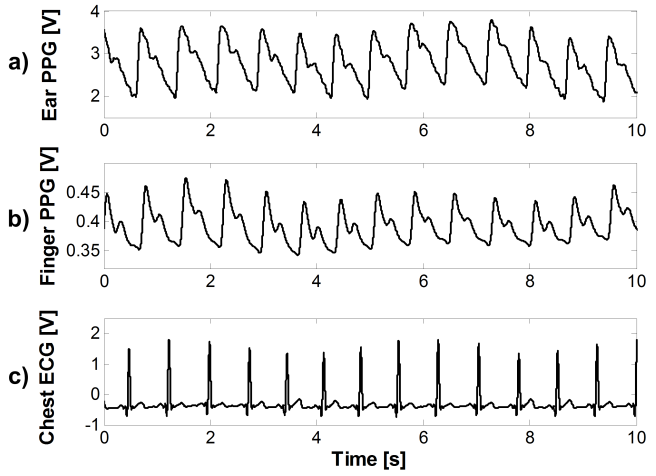

Fig. 2. a) Reflectance PPG behind the ear, b) transmission PPG at the finger, and c) chest lead II ECG.

III. BCG From Behind the Ear

To sense BCG at the ear, we use a hybrid electrode setup consisting of two capacitive electrodes for differential sensing, and one dry electrode for common-mode feedback (CMFB). Because the sensing electrodes are capacitive, their capacitances change with the mechanical vibrations associated with BCG, thus converting the mechanical movement to electrical signals. To reduce electrical interference, the capacitive electrodes are actively shielded. A dry electrode is used for CMFB. This avoids the skin irritation caused by wet electrodes and still maintains a low resistance feedback path to the body.

The electrodes are constructed using nylon fabric as the insulator and conductive nickel fabric as the conductor. Both fabric materials are suitable for comfortable long term wear. Photos of the electrodes and the construction materials are shown in Fig. 3.

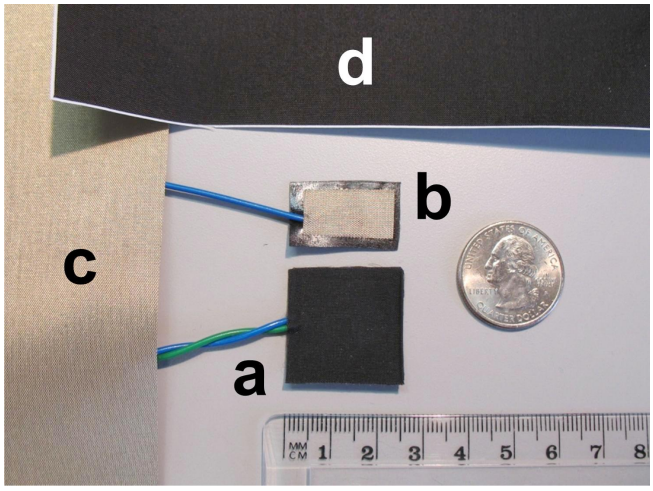

Fig. 3. Photo of a) the capacitive sensing electrode (25mm×25mm ×0.75mm), b) the dry CMFB electrode (15mm×25mm×0.35mm), c) the conductive fabric, and d) the nylon fabric.

Fig. 4 shows the 3D cross-section of the electrodes placed on skin. The capacitive sensing electrodes A and B have five layers consisting of a sensing layer, an active shield layer, and three insulating layers. The dry CMFB electrode is located between electrodes A and B and contains one layer driving CMFB signal into the body and one insulating layer.

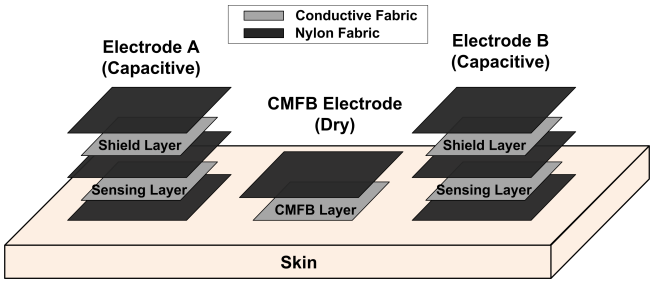

Fig. 4. 3D cross-section of the hybrid (capacitive and dry) electrode setup placed on skin, with conductive and insulating layers shown.

The diagram of the BCG front-end circuit is shown in Fig. 5. The capacitive electrodes have a capacitance to skin of approximately 4pF, or 4GΩ of reactance at 10Hz. Therefore, to minimize signal loss due to voltage division, the capacitive electrodes are connected to high impedance LMC6064 op amps ($I_{BIAS} = 10fA$) with 5GΩ bias resistors. The differential signal goes through two twin-T 60Hz notch filters and into an LT1920 instrumentation amplifier with a gain of 100. The common-mode signal is amplified by -200 and then fed back into the body to reduce signals such as 60Hz

interference. After the output, the signal is low-pass filtered in MATLAB with a cutoff frequency of 40Hz.

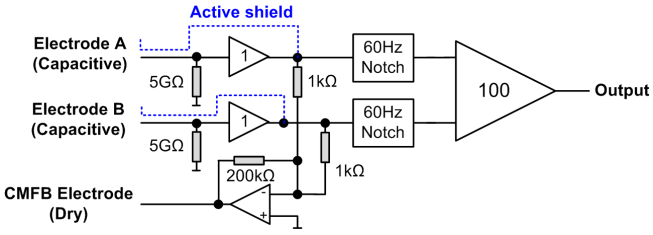

Fig. 5. The BCG front-end circuit diagram.

Using the hybrid electrodes and the front-end circuit, BCG is measured behind the right ear. For reference, a lead II chest ECG (wet electrodes) signal is simultaneously measured. Both signals are plotted in Fig. 6.

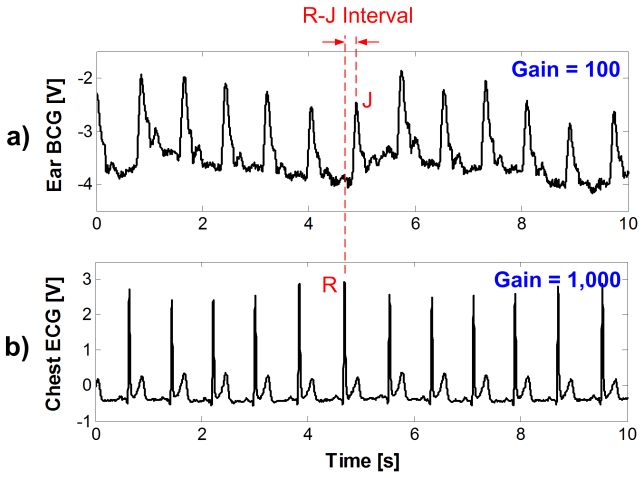

Fig. 6. a) BCG behind the ear and b) chest lead II ECG.

As shown in Fig. 6, the ear BCG has approximately ten times the signal strength of the chest ECG. The peak in the BCG is denoted as "J" by [10] and on average is 208ms±7.8ms after the R peak of the ECG (R-J interval). It should be noted that the J peak leads the PPG peak at the ear by approximately 40ms. Therefore, the BCG is not from local arterial pulsations at the ear. Furthermore, as shown by a longer measurement in Fig. 7, respiratory rate can also be extracted from the baseline oscillation of the BCG signal.

In Fig. 8, BCG is measured behind the ear while performing the Valsalva maneuver. The BCG's baseline drift is removed to clearly show amplitude change. Upon intrathoracic strain, the ventricular filling volume is decreased and cardiac output is reduced. This corresponds to the drop in the BCG amplitude. Upon release, the venous return is no longer impeded. Previously blocked blood rushes into the heart and increases ventricular filling volume, causing cardiac output to rise above the normal resting level. This is reflected in the elevated BCG amplitude after release.

Based on the PTT theory, blood pressure is inversely related to the delay between the R peak and the pulse arrival

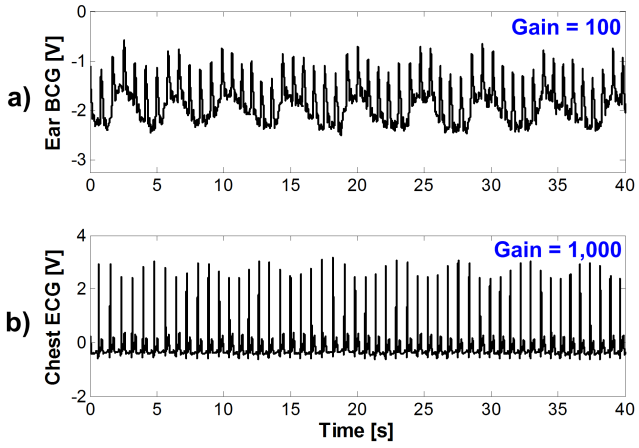

Fig. 7. a) BCG behind the ear and b) chest lead II ECG demonstrating respiration.

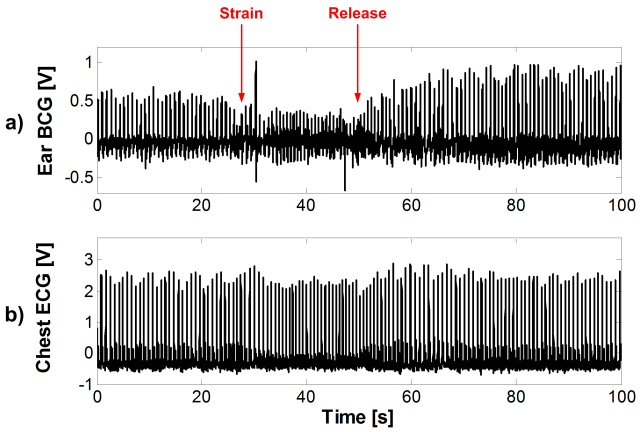

Fig. 8. Valsalva maneuver performed with a) BCG behind the ear and b) chest lead II ECG.

time at a location [7][8]. Fig. 9 plots the inverse of the R-J interval and heart rate during the Valsalva maneuver.

The numbered features of the waveforms in Fig. 9 are explained as follows:

1) Blood pressure varies with respiration. This can be seen in the oscillations in Fig. 9a.
2) As intrathoracic strain is applied, blood pressure rises rapidly as the applied intrathoracic pressure is directly translated to extrathoracic vessels. This peak is observed in Fig. 9a.
3) The continued intrathoracic pressure impedes venous return and reduces ventricular filling volume, causing a reduction in blood pressure. This drop is observed in Fig. 9a.
4) The drop in blood pressure stimulates the sympathetic nervous system, which slowly increases vasoconstriction and heart rate to restore blood pressure. This slow rise is observed in Fig. 9a, and the increased heart rate is seen in Fig. 9b.
5) The intrathoracic pressure is released and leads to a direct drop in transmural pressure of thoracic vessels

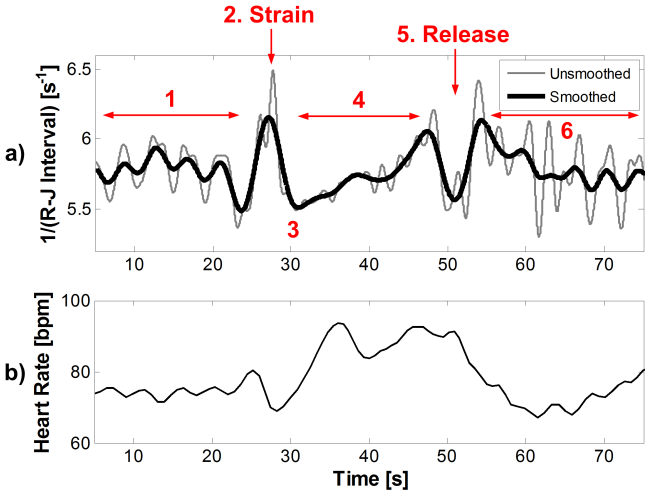

Fig. 9. a) The inverse of the R-J interval and b) heart rate during the Valsalva maneuver.

and an immediate drop in measured blood pressure. This dip is seen in Fig. 9a.

6) After a brief overshoot due to the increased stroke volume, blood pressure and heart rate return to normal. The waveforms in Fig. 9 also return to normal levels. Increased breathing oscillation is observed in Fig. 9a due to deeper breaths after the breath-hold maneuver.

In Fig. 10, a continuous Valsalva blood pressure measurement using a Portapres system is shown [16]. The mean arterial pressure in Fig. 10 displays all the marked features mentioned in Fig. 9a. Therefore, we confirm that the inverse of the R-J interval is correlated to blood pressure, which has also been reported in [17].

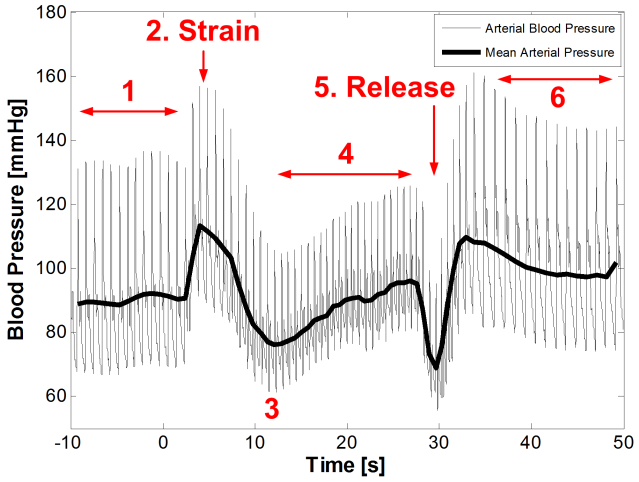

Fig. 10. Continuous blood pressure measured during the Valsalva maneuver using a Portapres system [16].

IV. Conclusion and Future Work

This work proposes the site behind the ear as a superior location for continuous and wearable vital signs monitoring. This location offers discreet sensing of reflectance PPG and BCG signals. PPG enables the measurement of blood oxygenation and heart rate, and BCG allows the measurement of heart rate and respiratory rate. With the Valsalva maneuver, it is shown that cardiac output is correlated to the amplitude of the BCG signal. Furthermore, when BCG is coupled with chest ECG, the inverse of the R-J interval correlates to blood pressure. Future work includes designing low noise circuits to sense ECG behind the ear to allow localized blood pressure estimation, and adding an accelerometer to enable orientation calibration.

V. Acknowledgments

The authors would like to thank Dr. Nathaniel Sims (MGH, HMS) and Dr. Collin Stultz (MIT) for their valuable discussions and insights.

References

[1] S. D. Pierdomenico, M. Di Nicola, A. L. Esposito, et al., "Prognostic value of different indices of blood pressure variability in hypertensive patients", *American Journal of Hypertension*, June 2009, pp. 842-847.

[2] Centers for Medicare & Medicaid Services, "Nation's health dollar," [Online]. Available: http://www3.cms.gov/NationalHealthExpendData/downloads/PieChartSourceExpenditures2008.pdf .

[3] National Institute for Health, "Improving heart failure disease management (R01)," Program Announcement Number PA-07-355, [Online]. Available: http://grants.nih.gov/grants/guide/pa-files/PA-07-355.html#PartI

[4] A. Searle and L. Kirkup, "A direct comparison of wet, dry and insulating bioelectric recording electrodes," *Physiol. Meas.*, vol. 21, pp. 271-283, 2000.

[5] B. Letac and P. Behar, "Variations in blood pressure at rest and during the day in 40 ambulatory hypertensive patients," *Arch. Mal. Coeur Vaiss.*, July 1986, pp. 1181-1187.

[6] B. P. McGrath, "Ambulatory blood pressure monitoring," *Med. J. Aust.*, vol. 176, no. 12, pp. 588-592, 2002.

[7] P. A. Shaltis, A. T. Reisner, and H. Asada, "Cuffless blood pressure monitoring using hydrostatic pressure changes," *IEEE Trans. On Biomedical Engineering*, vol. 55, no. 6, pp. 1775-1777, June 2008.

[8] K. Hung, Y. T. Zhang, and B. Tai, "Wearable medical devices for tele-home healthcare," *IEEE EMBC*, San Francisco, Sept. 2004, pp. 5384-5387.

[9] P. Shaltis, L. Wood, A. Reisner, and H. Asada, "Novel design for a wearable, rapidly deployable, wireless noninvasive triage sensor," *IEEE EMBC*, Shanghai, China, Sept. 2005, pp. 3567-3570.

[10] I. Starr, A. J. Rawson, H. A. Schroeder, and N. R. Joseph, "Studies on the estimation of cardiac output in man, and of abnormalities in cardiac function, from the heart's recoil and the blood's impacts; the ballistocardiogram," *The American Journal Of Physiology*, vol. 127, no. 1, pp. 1-28, Aug. 1939.

[11] O. T. Inan, M. Etemadi, R. M. Wiard, L. Giovangrandi, and G. T. A. Kovacs, "Robust ballistocardiogram acquisition for home monitoring," *Physiological Measurement*, vol. 30, no. 2, Feb. 2009.

[12] T. Koivistoinen, S. Junnila, A. Vrri, and T. Kbi, "A new method for measuring the ballistocardiogram using EMFi sensors in a normal chair," *IEEE EMBC*, San Francisco, Sept. 2004, pp. 2026-2029.

[13] B. H. Jansen, B. H. Larson, and K. Shankar, "Monitoring of the ballistocardiogram with the static charge sensitive bed," *IEEE Trans. On Biomedical Engineering*, vol. 38, no. 8, Aug. 1991.

[14] D. G. Guo, F. E. H. Tay, L. Xu, et al., "A long-term wearable vital signs monitoring system using BSN," *IEEE Euromico Conf. on Dig. Sys. Des. Arch*, Italy, Sept. 2008, pp. 825-830.

[15] P. C. Branche, W. S. Johnston, C. J. Pujary, and Y. Mendelson, "Measurement reproducibility and sensor placement considerations in designing a wearable pulse oximeter for military applications," *IEEE Bioengineering Conf.*, Apr. 2004, pp. 216-217.

[16] T. Heldt, "Computational models of cardiovascular response to orthostatic stress," Ph.D. dissertation, Harvard-MIT Division of Health Sciences and Technology, Cambridge, MA, 2004.

[17] J. Shin, K. M. Lee, and K. S. Park, "Non-constrained monitoring of systolic blood pressure on a weighing scale," *Physiological Measurement*, vol. 30, no. 7, July 2009.